



Effects of mean net stress and cyclic deviatoric stress on the cyclic behavior of normally consolidated unsaturated kaolin

M. Mojezi¹, M.K. Jafari^{2,*}, M. Biglari³

Received: May 2015, Revised: July 2015, Accepted: August 2015

Abstract

Experimental study of the cyclic behavior of unsaturated materials is more complex than that of the saturated materials due to the required equipment, experience and time. Furthering investigations in the field of unsaturated materials is necessary to better understand its complexity and sensitivity of unsaturated cyclic parameters to different determinants such as suction path, stress path, loading speed, deviatoric stress amplitude, physical specifications, and etc. To this end, the main focus of this study has been to analyze the effects of factors such as mean net stress and deviatoric stress levels in fast cyclic loading on the cyclic behavior of a normally consolidated unsaturated fine-grained trade soil, namely the Zenoz kaolin. Various unsaturated tests were performed in three mean net stress levels and three amplitudes of cyclic deviatoric stress levels. Results showed that increase of suction in the same strain level leads to increase in stiffness in normally consolidated samples (i.e. increase in elastic modulus and shear modulus and decrease in damping ratio). Also, in the same suction value and strain level, increase of the mean net stress during the isotropic consolidation causes to the denser normally consolidated samples and results to increase of elastic modulus and shear modulus, and decrease of damping ratio.

Keywords: Cyclic loading, Unsaturated, Zenoz kaolin, Mean net stress, Deviatoric stress amplitude, Suction controlled-cyclic triaxial.

1. Introduction

In the past few decades, experimental researches on the study of unsaturated soils behavior faced many limitations. These limitations were mainly due to a lack of proper equipment needed for such investigations. However, in recent years, new developments in the field of the promoted laboratory equipment have led to valuable discoveries in the recognition of some behavioral aspects of this kind of materials. Most of the above-mentioned discoveries have been limited to assessing and formulating the static behavior and volumetric changes of unsaturated materials. Furthermore, recent advances in the dynamic and cyclic suction controlled equipment have led to the generation of data in the new modeling of the dynamic behavior of unsaturated soils in the range of small strains. Experimental studies have shown that the initial shear modulus (G_0) of unsaturated soils is affected by the applied stress and suction levels.

In addition, the latest researches on the measurement of the shear modulus of unsaturated soils in the range of medium to large strains using suction controlled cyclic triaxial apparatus have shown that strain-dependent normalized shear modulus reduction and damping ratio curves ($G-\gamma$ and $D-\gamma$ curves) are influenced by changes in the suction level.

Cyclic or dynamic behavior of soils is usually described using parameters such as shear modulus (G) and Damping ratio (D) or by shear modulus reduction and damping ratio curves. Also, to calculate the shear modulus in a triaxial test, the elastic modulus (E) of the specimen must be measured. As earlier mentioned, due to the difficulties present in the testing of unsaturated soils there is a lack of sufficient experimental data in this field. So the unsaturated constitutive and parametric models, which are suggested by researchers to now, are not general and complete models. Mentioned data consist of dynamic and cyclic parameter values obtained from various kinds of unsaturated soils (G_0 , G , D , G/G_0). Changes within these parameters occur due to factors such as suction, mean net stress, deviatoric stress, cycle quantity, and etc. So in this paper the effects of some mentioned factors have been investigated on cyclic parameters of a fine-grained soil. Numerous tests must be run on different stress path, loading conditions, and sample preparation methods to determine the complete and general behavior of any kind of soil.

* Corresponding author: jafari@iiees.ac.ir

1 Ph.D. Candidate, International Institute of Earthquake Engineering and Seismology, Tehran, Iran

2 Professor, International Institute of Earthquake Engineering and Seismology, Tehran, Iran

3 Assistant Professor, Razi University, Kermanshah, Iran

Several researchers investigated on the impact of matric suction variable on dynamic parameters of unsaturated materials (mostly in small strains). Among them Marinho et al. [1] can be mentioned who measured the shear wave velocity in some samples of London clay using the bender element method. Also, Picornell & Nazarian [2], by some measurements using the bender element on reconstituted fine and coarse granular samples, found that G_0 increases and reaches a boundary value by increased suction. Cabarkapa et al. [3] obtained the stiffness of a kind of silt with sharp corners in the triaxial cell, which applies the suction controlled condition, using bender element. Mancuso et al. [4] by presenting the results of experiments performed in the resonant column-torsional shear (RCTS) and unsaturated triaxial apparatus on a type of silty sand soil, showed that soil structure has caused significant changes on the stiffness. Vassallo & Mancuso [5] focused on laboratory evidences for the behavior in large strains, and calculated the stiffness of the silty sand in large strain ranges. Vassallo et al. [6,7] examined the effects of the history of net stress and suction on the stiffness of silty clay soils in the range of small strains, and modeled the behavior in compacted silts. Becker & Meissner [8], tried to develop the elasto-plastic behavior model, based on the experimental results, using the effective stress assumption. Becker & Li [9], carried out experiments on reconstituted samples using a triaxial apparatus and an unsaturated consolidation apparatus in which a small tensiometer was applied. Mendoza et al. [10], studied the stiffness of compacted unsaturated clayey soils in very small strains as well as the effect of wetting on stiffness and Young's modulus. Cabarkapa and Cuccovillo [11] studied the hydromechanical behavior of unsaturated non-plastic quartz silt by making two automatic triaxial apparatuses. Ng & Yung [12] measured the shear wave velocity in different directions in a type of clayey silt using a developed triaxial apparatus equipped with three pairs of bender element. Pineda et al. [13] investigated the wetting and drying effects on the shear stiffness in a type of clayey silt in small strains using two different techniques, bender element and resonant column. d'Onza et al. [14] evaluated the effects of the mean net stress and suction on the initial shear stiffness (G_0) and initial damping ratio (D_0) of two material types, the clayey silt and compacted silty sand, at optimum water content condition. Ng et al. [15] in their study investigated the wetting-drying effects and stress ratio on anisotropy in the shear stiffness of an unsaturated clayey silt at very small strains. Biglari et al. [16] studied the shear modulus and damping ratio of unsaturated Zenoz kaolin materials using improved suction controlled triaxial apparatus at medium to large strains in constant suction condition during slow loading cycles. Biglari et al. [17] carried out an experimental study to investigate the effects of isotropic compression, wetting and drying on the initial shear stiffness of an unsaturated lean clay, both in normally consolidated and over consolidated conditions using fixed-free resonant column – torsional shear (RCTS). Ng & Xu [18] investigated the effects of suction history on both the very small-strain shear modulus (G_0) and shear modulus reduction curve of an unsaturated soil, by carrying out constant mean net stress compression

triaxial tests with bender elements and local strain measurements. Heitor et al. [19] presented an experimental study on the small-strain behavior of compacted silty sand prepared with varying initial moisture contents and compaction energies, which were tested with bender elements to determine the small strain shear modulus (G_0), while the post compaction matric suction was measured using the filter paper method and tensiometer. Surlol et al. [20] studied the small strain shear modulus of compacted Barcelona silty clay data at different confining stresses using a resonant column apparatus. They focused on the effects of the initial state and the microstructure set on compaction, covering a wide range of saturation degrees. Walton-Macaulay et al. [21] did an experimental program to investigate the possible uniqueness of the small-strain shear modulus surface using a modified resonant column apparatus. They concluded that a unique relationship exists between small-strain shear modulus, matric suction, and mean net stress.

In this research, the effects of mean net stress level and deviatoric stress amplitude in fast cyclic loading at constant water content conditions were studied in order to simulate earthquake loading conditions, using suction controlled cyclic triaxial apparatus improved by Biglari et al. [16]. These devices are able to make programmable measurements and monitor the changes in suction, mean net stress, and deviatoric stress. Several tests have been conducted on normally consolidated samples of unsaturated Zenoz kaolin, which are prepared with the same initial condition. The results are presented in the following.

2. Equipment

The tests planned in this research were performed using the suction controlled cyclic triaxial apparatus (Fig. 1). This apparatus consists of different parts, which are managed and planned as uniform and programmable by a computer control system. These parts can apply and measure axial and confining stresses, pore water pressures and pore air pressures. The suction controlled cyclic triaxial apparatus can also measure the samples' axial and volumetric deformations.

Axial, confine, pore water and pore air pressures in this system are applied through an air pressure source with a maximum pressure of 1 MPa. The pressure control is performed by four electro-pneumatic convertors. Axial pressures can be measured by means of a load cell with a capacity of 5 kN above the top cap. In addition, confine, pore water and pore air pressures are measured by three pressure transducers. Changes in the volume of pore water and volume of the sample submerged in an environmental water bath of the sample can be determined via two differential pressure transducers.

The axial translation technique proposed by Hilf [22] is used to control the suction. Axial deformations of the specimen are measured using a linear variable differential transformer (LVDT) (in the range of 50 mm and accuracy of 0.1%) located out of the cell and a gap sensor (in the range of 8 mm and accuracy of 0.02 %) located inside the cell.

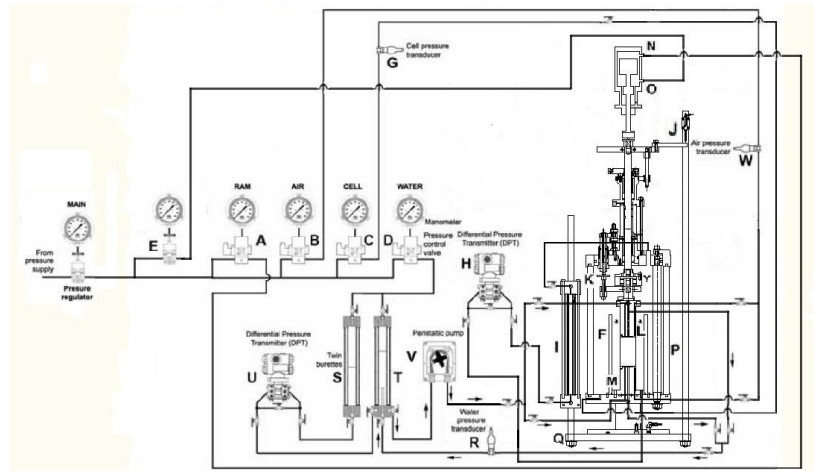


Fig. 1 suction controlled cyclic triaxial apparatus [16]

Volumetric changes of the sample are determined by controlling the changes in water level around the sample and water level in a reference burette using a differential pressure transducer (DPT). For this purpose, the cell pressure (applied to the reservoir of the water around the sample), is necessary to be the same as the reference burette. This is achieved through high association of the two compartments. To prevent evaporation or infiltration of air bubbles into the reservoir water and the burette reference water, a layer of silicone oil is placed on water surfaces in these reservoirs. Additionally radial deformation of the samples can be determined by volume changes and axial deformations.

In order to minimize the effect of ambient temperature on the results, all the tools have been placed in the isolation chamber at a constant temperature of 22 °C during testing.

Due to the long-time experiments, very small air bubbles may be trapped in the drainage system beneath the ceramic discs. These bubbles may lead to errors in the estimation of water content of the samples. To handle this problem, a pump is installed in the system, and by turning

it on in appropriate time scales, these air bubbles are pushed out from the drainage system. The data can be modified by measuring volume of the air exited during each period.

Man-made errors affecting these tests may be due to sample construction and its set up to the apparatus. Therefore, high precision is necessary in the initial stage of this process. After setting up the specimens, all stress path stages are controlled and recorded by a computer, which reduces man-made error during test procedures.

3. Materials Tested

The material used in this study was Zenoz kaolin with specifications presented in Table (1). Firstly, an amount of this soil is placed and dried in a desiccator beside the silica gel for over a few days. Dried soil is then mixed with particular amounts of distilled water, and water content equalization is achieved in a sealed glass container within 16 to 24 hours.

Table 1 Properties of the tested soils

| Classification | CL |
|---|------|
| Clay Fraction (%) | 18 |
| Silt Fraction (%) | 60 |
| Plasticity Index: PI (%) | 12 |
| Liquid Limit: LL (%) | 29 |
| Plastic Limit: PL (%) | 17 |
| Specific Gravity: G_s | 2.65 |
| Optimum Water Content: ω_{opt} (%) | 15.4 |
| Maximum Dry Unit Weight: $\gamma_{d(max)}$ (g/cm ³) | 1.74 |
| Initial Void Ratio: e_0 | 1.19 |
| Initial Degree of Saturation: Sr_0 (%) | 27 |

The samples have been compacted and prepared by the under-compaction method proposed by Ladd [23] in a cylindrical shape of 38 mm in diameter and 76 mm in height. In order to achieve a normally consolidated condition the samples are made with 11.9 % water content (3.5% less than the optimum water content) and dry unit weight of 12 kN/m³ (69 % of the maximum dry unit weight, obtained by the standard proctor test).

4. Test Procedures and Results Before Cyclic Loading

Regarding the objectives included in this study, the tests in this study have been planned and executed in three mean net stress levels of 100, 200, and 300 kPa (named M100, M200, and M300) and two suction levels of zero and 150 kPa (named S0 and S150). The general test

procedures included sample preparation, sample installment, initial equalization, isotropic consolidation in constant suction, two-way cyclic loading at three deviatoric stress amplitudes of 18, 42, and 81kPa (named D18, D42, and D81) with any mean net stress and suction level in 40 to 60 cycles, as well as monitoring and recording the data of the axial and deviatoric loads, mean net stress, suction, pore water pressure, pore air pressure,

and sample deformations. Since the suction condition is disrupted after applying deviatoric stress cycles in rapid loading, separate samples are tested for every deviatoric stress amplitudes. Constant factors before applying the cycles for all samples include the construction conditions, initial equalization, isotropic consolidation, and loading paths. Fig. 2 shows a simplified version of the test stress paths, and in Table 2 illustrates these paths in more detail.

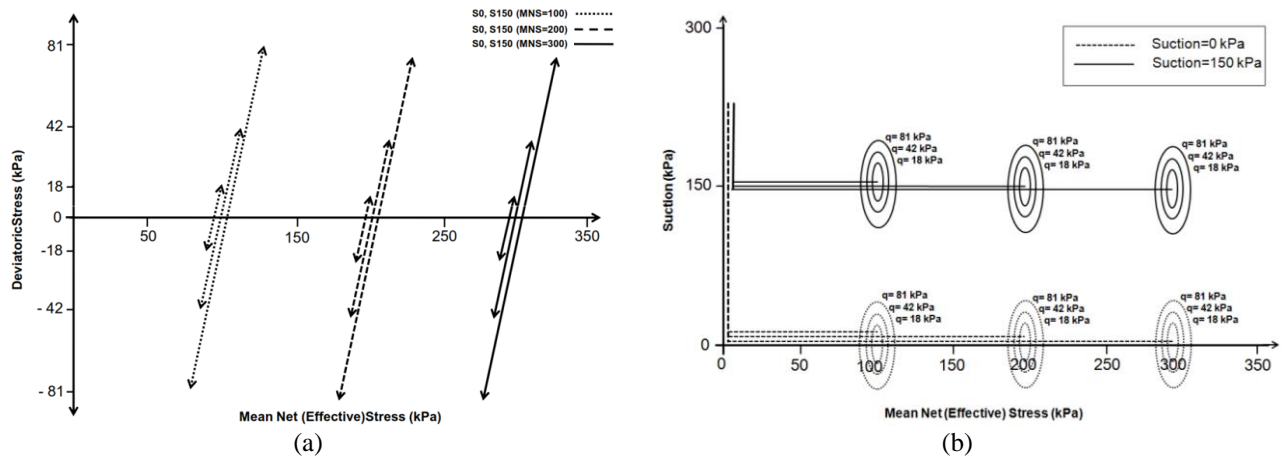


Fig. 2 stress paths in the tests (a): deviatoric stress versus mean net stress (b): suction versus mean net stress

Table 2 Details of stress paths

| No. | Test (Sample) Name | end of Initial Equalization | | | end of Isotropic Consolidation (before Cyclic Loading) | | | | | Cyclic Amplitude (kPa) |
|-----|--------------------|--------------------------------|----------------------------------|-------------------------------------|--|----------------------------------|-------------------------------------|---------------|-----------------------|------------------------|
| | | Pore Air Pressure: u_a (kPa) | Pore Water Pressure: u_w (kPa) | Stress: $\sigma_1 = \sigma_3$ (kPa) | Pore Air Pressure: u_a (kPa) | Pore Water Pressure: u_w (kPa) | Stress: $\sigma_1 = \sigma_3$ (kPa) | Suction (kPa) | Mean Net Stress (kPa) | |
| 1 | S0M100D18 | --- | 50 | 55 | --- | 50 | 150 | 0 | 100 | 18 |
| 2 | S0M100D42 | --- | 50 | 55 | --- | 50 | 150 | 0 | 100 | 42 |
| 3 | S0M100D81 | --- | 50 | 55 | --- | 50 | 150 | 0 | 100 | 81 |
| 4 | S0M200D18 | --- | 50 | 55 | --- | 50 | 250 | 0 | 200 | 18 |
| 5 | S0M200D42 | --- | 50 | 55 | --- | 50 | 250 | 0 | 200 | 42 |
| 6 | S0M200D81 | --- | 50 | 55 | --- | 50 | 250 | 0 | 200 | 81 |
| 7 | S0M300D18 | --- | 50 | 55 | --- | 50 | 350 | 0 | 300 | 18 |
| 8 | S0M300D42 | --- | 50 | 55 | --- | 50 | 350 | 0 | 300 | 42 |
| 9 | S0M300D81 | --- | 50 | 55 | --- | 50 | 350 | 0 | 300 | 81 |
| 10 | S150M100D18 | 200 | 50 | 250 | 200 | 50 | 300 | 150 | 100 | 18 |
| 11 | S150M100D42 | 200 | 50 | 250 | 200 | 50 | 300 | 150 | 100 | 42 |
| 12 | S150M100D81 | 200 | 50 | 250 | 200 | 50 | 300 | 150 | 100 | 81 |
| 13 | S150M200D18 | 200 | 50 | 250 | 200 | 50 | 400 | 150 | 200 | 18 |
| 14 | S150M200D42 | 200 | 50 | 250 | 200 | 50 | 400 | 150 | 200 | 42 |
| 15 | S150M200D81 | 200 | 50 | 250 | 200 | 50 | 400 | 150 | 200 | 81 |
| 16 | S150M300D18 | 200 | 50 | 250 | 200 | 50 | 500 | 150 | 300 | 18 |
| 17 | S150M300D42 | 200 | 50 | 250 | 200 | 50 | 500 | 150 | 300 | 42 |
| 18 | S150M300D81 | 200 | 50 | 250 | 200 | 50 | 500 | 150 | 300 | 81 |

4.1. Initial equalization stage

Once the sample is placed in the cell, while observing certain precautions to prevent disturbance during installation, the samples are brought to suction equalization condition. This process is performed in the tests with suction of 150 kPa (S150) by a gradual and appropriate application of the axial and confined pore water and pore air pressures, up to the predetermined values, and fixing the suction at 150kPa.

Also, in zero-suction (S0) tests, by applying CO₂ then de-aired distilled water, the samples have brought to the

saturated condition, and the saturation is controlled by Skempton's B parameter. During the initial equalization stage, the specific volume changes and specific water volume are controlled to achieve equalization. According to Sivakumar [24], in the case that the changes in water content become less than 0.04 % per day, the sample has reached suction equalization. Fig. 3 illustrates the specific volume changes, as an instance, for S0M300 and S150M300 tests, while Fig. 4 shows the specific water volume changes for S150M100 and S150M300 tests during initial equalization stage in three amplitudes of cyclic deviatoric stress levels. Changes in these parameters have

shown similar trends in other tests leading way to similar results. In the tests with zero suction level changes in water volume during equalization that have been affected by the saturation process, have not been illustrated here due to the complexity it can cause in the concepts and the results of the tests carried out under 150 kPa suction level.

The diagrams relating to S150 tests in Fig. 4 illustrate water content absorption in the sample during the equalization stage. This indicates that the initial suction of the constructed samples has been in an upper level compared to the suction of 150kPa.

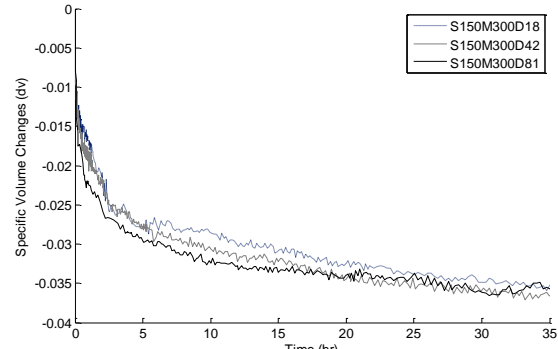
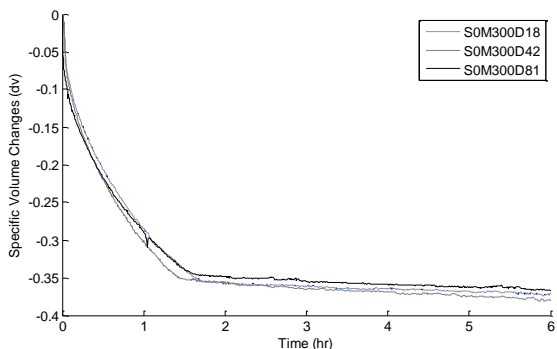


Fig. 3 Specific volume changes during initial equalization for SOM300 and S150M300 tests

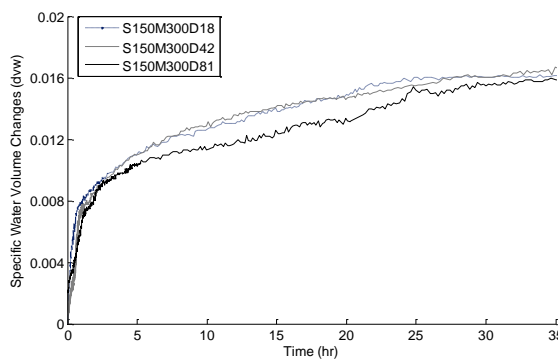
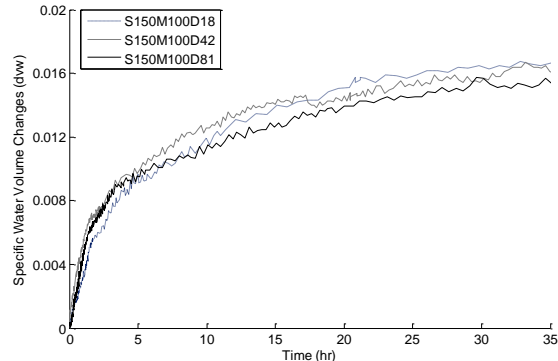


Fig. 4 Specific water volume changes during initial equalization for S150M100 and S150M300 tests

4.2. Isotropic consolidation stage

During loading process, and after the initial suction equalization, a confined stress with the rate of 8 kPa/h is applied, and the samples are consolidated isotropically in a fixed suction to arrive at the determined mean net stress (100, 200, and 300 kPa).

In Figs. 5 and 6, specific volume and specific water volume changes are presented versus the mean net stress during the isotropic consolidation stage for tests S0D81 and S150D81 in three amplitudes of cyclic deviatoric stress. The changes showed similar trends for other tests,

thereby proving its accuracy. As shown in Fig. 5, reduction of the specific volume in S0 samples is more significant than in the S150. This can be due to the collapse of the samples in S0 tests due to the fast entrance of water in the samples with zero-suction equalization stage. The curves show that the predetermined mean stress levels for the cyclic loading (100, 200 and 300 kPa) are higher than the pre-consolidated stress induced to the samples (resulted from their construction stages), thereby ensuring that the loading cycles have been executed in normally consolidated conditions.

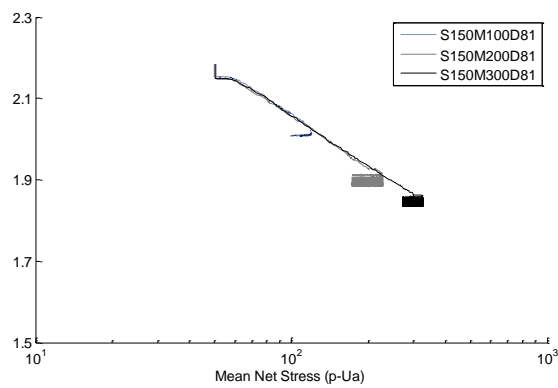
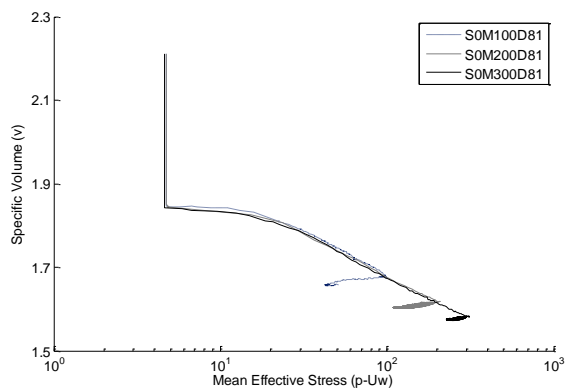


Fig. 5 Specific volume changes during isotropic consolidation for S0D81 and S150D81 tests

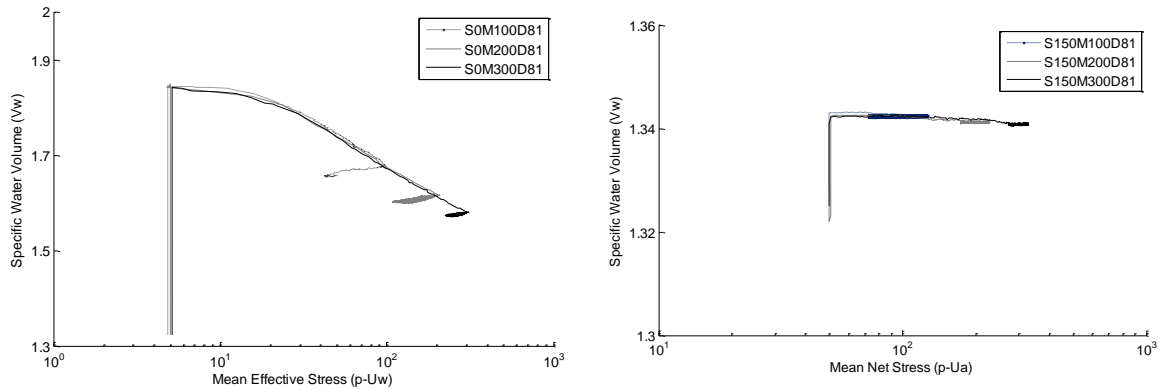


Fig. 6 Specific water volume changes during isotropic consolidation for S0D81 and S150D81 tests

4.3. Two-way deviatoric stress cycles

By achieving the predetermined mean net stresses to applying cyclic loading, the drainage valves are initially closed, the recording time is set for one record per second, the gap sensor is adjusted to zero, and finally the cyclic loading program is imposed up to the predetermined deviatoric stress amplitudes (18, 42, and 81 kPa, for every separate sample of the same initial condition) with the frequency of 0.003 Hz. The paths covered during the tests are shown schematically in Fig. 2.

5. Results after Cyclic Loading

Following, the results of applying two-way deviatoric stress cycles in different conditions of stress and suction are presented. It should be mentioned that loading cycles have been carried out up to 40 cycles in tests with zero suction and mean net stress of 100kPa, and up to 60 cycles in other tests. In some tests, the cyclic loading path is stopped in fewer cycles. To achieve normally consolidated conditions, the samples are prepared under dryer conditions as opposed to the optimum water content, and with a unit weight of less than the maximum dry unit weight. Regarding the weakness of the samples, the stop of the loading can be due to the failure of the sample resulting from the speed or rate of the loadings. The tests are named as S-M-D in which S introduces the suction, M indicates the mean net stress, and D represents the deviatoric stress. The numbers after these letters give the related stress value in kPa.

In Fig. 7, for example, the changes in deviatoric stress versus the axial strain have been presented for suction levels of zero and 150 kPa in the tests with mean net stress of 200kPa and deviatoric stress of 81kPa. In the test SOM200D81, 60 cycles of loading have been carried out but the test S150M200D81 has been stopped after 23 cycles. The accuracy and stability of the performed two-way cyclic loadings can be deduced from the results of this figure.

Changes in pore water pressure during cyclic loading are illustrated in Fig. 8, as an instance, for two series of the tests with the same stress path but different suction levels of 0 and 150 kPa (SOM300D18,42,81 and S150M300D18,42,81 tests). In both series of the tests, the pore water pressure was increased for all of the deviatoric stress levels, and the range of these changes has been raised as the deviatoric stress amplitude increased. Though it is interesting that in the tests with zero suction level, the pore water pressure changes were located at higher levels, and were increased in an oscillatory trend simultaneous to the cyclic deviatoric stress loading. The tests with a suction of 150 kPa however, showed that the changes of pore water pressure versus time was approximately linear, and increased at lower levels. This observation clarifies that specimens related to the zero suction tests had been saturated prior to applying cyclic loading, the deviatoric stress loading cycles apply to fully saturated specimens, but in tests with a suction level of 150 kPa the loading applies to unsaturated samples with air voids inside. These air voids release parts of the cyclic loading, and prevent pore water pressure to change oscillatory.

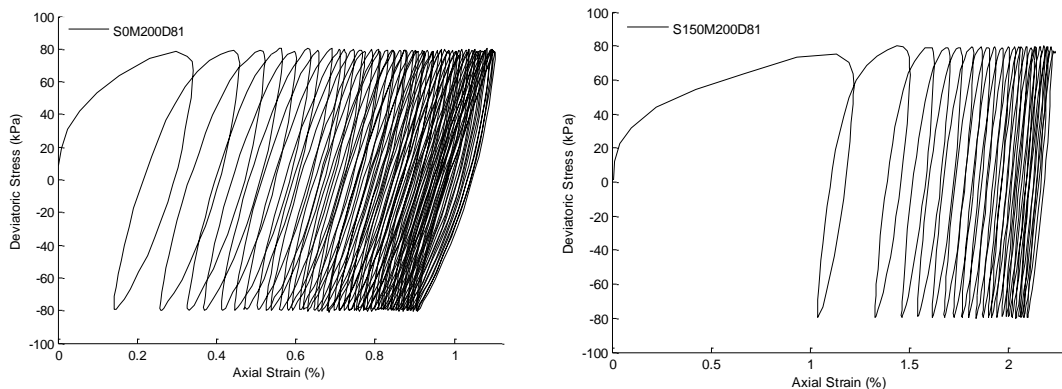


Fig. 7 Deviatoric stress versus axial strain in tests SOM200D81 and S150M200D81

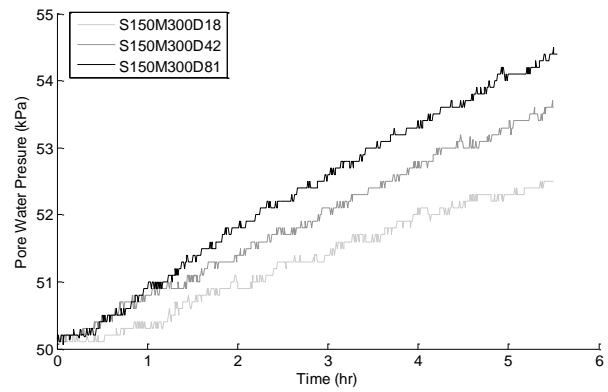
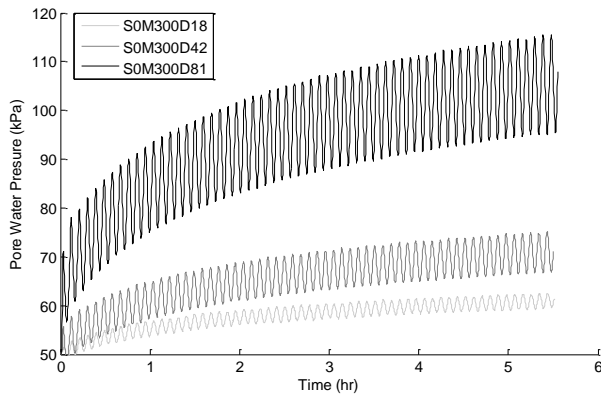


Fig. 8 pore water pressure changes during loading cycles for SOM300 and S150M300 tests

The shear modulus (G) was calculated with equation $G = E / (2(1 + \nu))$. In this equation, E , Young's modulus, was determined as the ratio between the peak-to-peak deviatoric stress and the peak-to-peak axial strain along each cycle; and ν , poisson's ratio, which was calculated from the ratio of measured radial and axial strains. According to Fig. 9, damping ratio (D), was calculated with equation $D = W_D / (4\pi \cdot W_S)$, where W_D is the area of the hysteresis loop and W_S is the area of the hatched triangle.

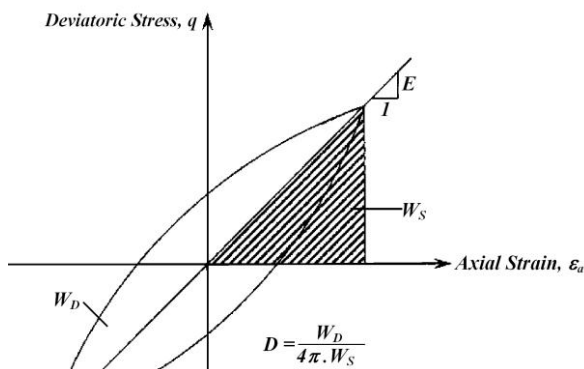


Fig. 9 Determination of elastic modulus and damping ratio in cyclic triaxial test

In the graphs presented for the dynamic parameters (Figs. 10 through 12), because of the intensity of the data relating to the cycles, the results for cycles 1, 3, 5, 10, 15, 20, ..., 60 are shown. In addition, the values related to the first loading cycles are connected by dashed lines (for S0 tests) and by solid lines (for S150 tests). It must be mentioned that in the tests M300D81 (the mean net stress of 300 kPa and deviatoric stress amplitude of 81 kPa), due to the high amplitude of the deviatoric stress on the one hand, and looseness of the made sample in the initial

condition on the other hand, the sample had failed after the first loading cycle. Therefore at this level of the mean net stress and deviatoric stress amplitude, in the test S0 (zero suction) only one data related to the first cycle is obtained, and in the test S150 (suction of 150 kPa), the sample had failed during the first loading cycle, and hence, no data is achieved from this test.

The significant effects of suction on the evaluated dynamic parameters can be deduced from the graphs presented in Figs. 10 through 12. In all three mean stress levels of 100, 200, and 300 kPa, in the same strain levels, elastic and shear modulus parameters (E and G) at the suction value of 150 kPa were increased relative to their corresponding values of zero suction, while the damping ratio (D) was decreased. This suggests that enhancement of suction has caused to increase in stiffness by inducing a virtual cohesion between the sample particles.

A comparison between the curves for the same suction levels and same strain levels shows that rise of the mean net stress has led to increase in shear modulus, and has decreased damping ratio. This is due to the increased compaction of the samples resulting from the isotropic consolidation in the strain levels prior to the application of the cycles. Increased compaction can be viewed in Fig. 5, which indicates the decrease in specific volume occurs as mean stress levels increase. This finding had a fairly similar trend for both suction values of zero and 150 kPa, but the changes were greater in the suction of 150 kPa.

Raising the number of cycles for any deviatoric stress amplitude would increase the elastic modulus and shear modulus, but decrease the damping ratio. Referring to Fig. 4, it is observed that raising the number of cycles would result in the specific volume decrease. This volume reduction has consequently led to increased stiffness, and hence the higher elastic modulus and shear modulus, and decrease in damping ratio.

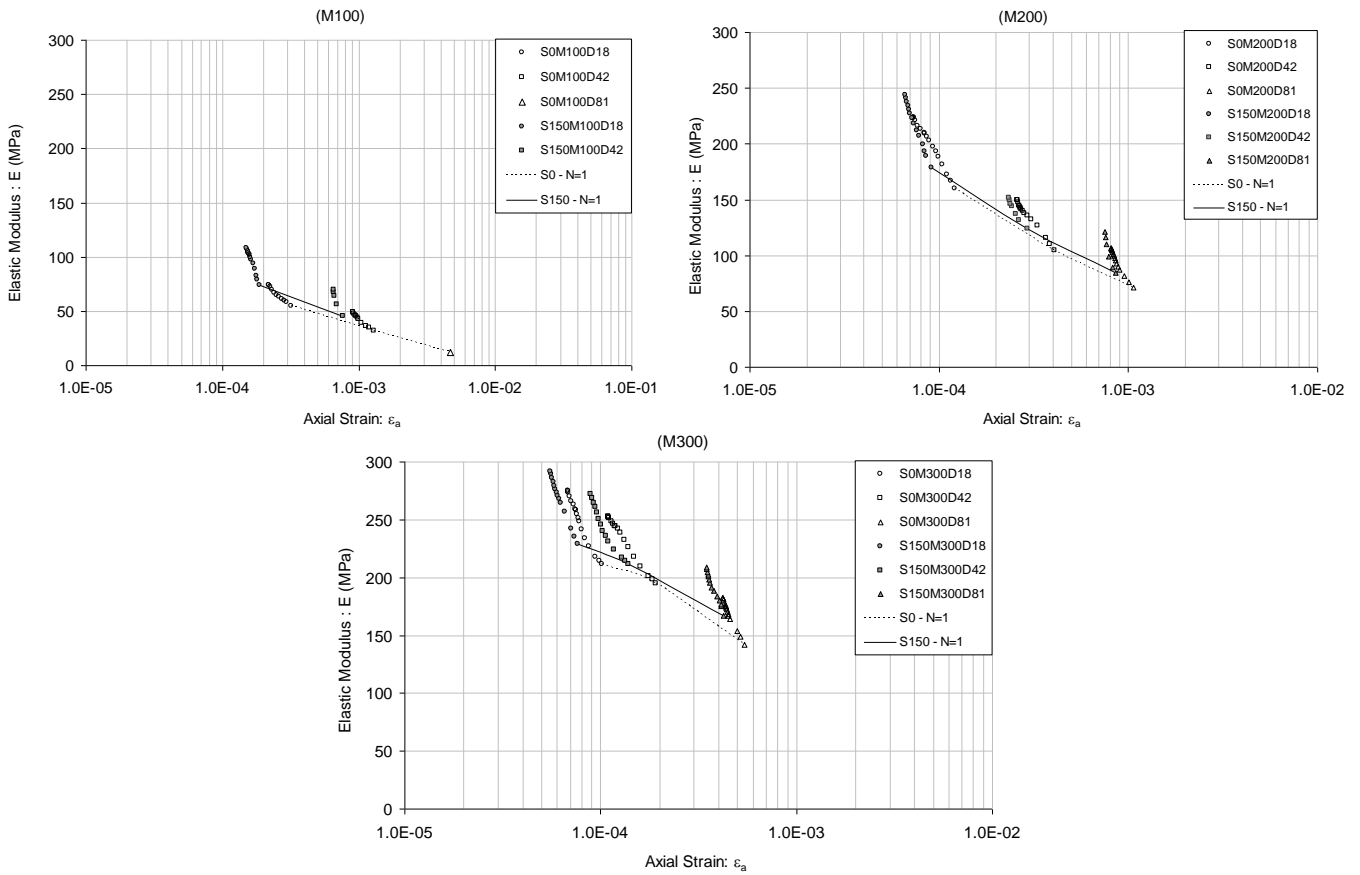


Fig. 10 Changes of elastic modulus versus axial strain for mean net stress levels of 100, 200 and 300 kPa

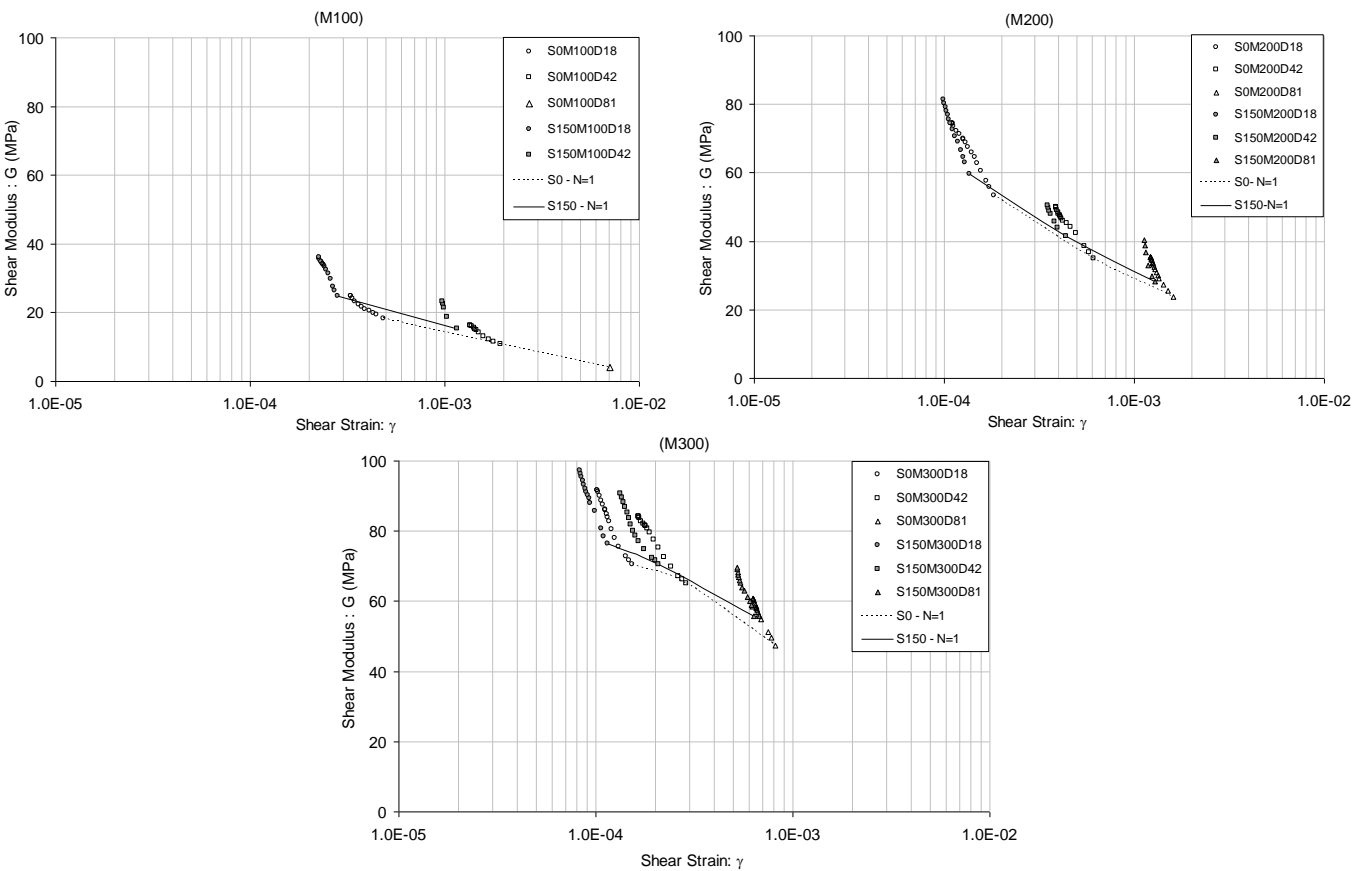


Fig. 11 Changes of shear modulus versus shear strain for mean net stress levels of 100, 200 and 300 kPa

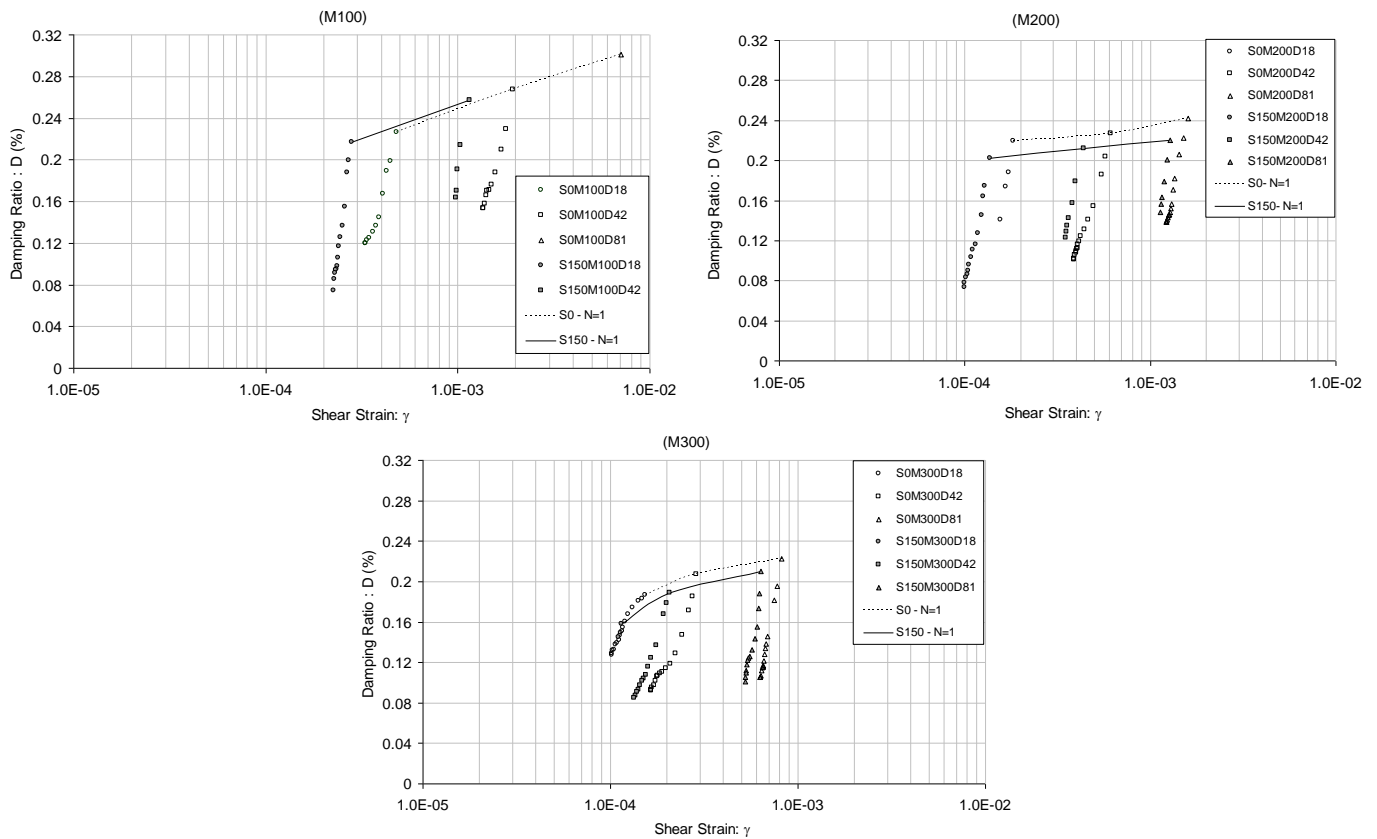


Fig. 12 Changes of damping ratio versus shear strain for mean net stress levels of 100, 200 and 300 kPa

6. Conclusion

In this research, the results obtained from the suction controlled cyclic triaxial tests on samples with the same initial conditions on Zeno kaolin soil, a fine-grained clayey material, were presented to study the effects of suction and mean net stress on the parameters of the elastic modulus, shear modulus and damping ratio. These materials have been studied in unsaturated normally consolidated conditions. The results suggest that mean net stress and suction have significant effects on the dynamic parameters of unsaturated clayey samples. Increase of suction, up to the levels investigated in this study, in the same strain levels leads to increase of the samples stiffness and results to increase in the elastic modulus and the shear modulus and decrease in the damping ratio. Also, in particular levels of suction and strain, increase in the mean net stress during the isotropic consolidation results in more compacted samples, and leads to a rise in the elastic modulus and the shear modulus, and reduction in the damping ratio.

Furthermore, the findings indicate that by increased deviatoric stress amplitude in the same mean net stress level and the same number of cycles, the parameters E and G have reduced and parameter D has increased.

In general, it can be concluded that in the same mean net stress levels or the equal suction levels, by increasing the shear strain level, the values of the elastic modulus and shear modulus have decreased and the damping ratio has increased. On the other hand, increase of the cycles number for all mean net stress levels and suctions, by inducing the increased stiffness as a result of decreased sample volume,

followed by the enhancement of elastic modulus and shear modulus, and decrease of the damping ratio.

Finally it is concluded that according to the considerable effects of suction on the soil's cyclic behavior on the one hand and the influence of various parameters such as mean net stress, deviatoric stress amplitude and number of cycles on the behavior of unsaturated soils on the other hand, it is necessary to fully consider these effects in research pertaining to the modeling the behavior of unsaturated materials, and to suggest proper unsaturated constitutive models. This would require increased studies and data production in this field of the science.

References

- [1] Marinho EAM, Chandler RJ, Crilly MS. Stiffness measurements on a high plasticity clay using bender elements, In *Unsaturated Soils, Proceedings of the First International Conference on Unsaturated Soils, UNSAT 95, Paris, France, AA Balkema, Rotterdam, 1995, Vol. 1, pp. 535-539.*
- [2] Picornell M, Nazarian S. Effects of soil suction on low-strain shear modulus of soils, *Proceedings of Second International Conference on Unsaturated Soils, August 27-30, Beijing, China, 1998, Vol. 1, pp. 102-107.*
- [3] Cabarkapa Z, Cuccovillo T, Gunn M. Some aspects of the pre-failure behavior of unsaturated soil, *Proceedings of second international conference on prefailure behavior of geomaterials, Torino, 1999, pp. 159-165.*
- [4] Mancuso C, Vassallo R, d'Onofrio A. Soil behaviour in suction controlled cyclic and dynamic torsional shear tests, *Proceedings of the Asian Conference on Unsaturated Soils, Singapore, 2000, Vol. 1, pp. 539-544.*

- [5] Vassallo R, Mancuso C. Soil behaviour in the small and the large strain range under controlled suction conditions, International Workshop on Experimental Evidence and Theoretical Approaches in Unsaturated Soils, Toronto, 2000, pp. 75-90.
- [6] Vassallo R, Mancuso C, Vinale F. Effects of net stress and suction history on the small-strain stiffness of a compacted clayey silt, Canadian Geotechnical Journal, 2007, Vol. 44, pp. 447-462.
- [7] Vassallo R, Mancuso C, Vinale F. Modelling the influence of stress-strain history on the initial shear stiffness of an unsaturated compacted silt, Canadian Geotechnical Journal, 2007, Vol. 44, pp. 463-472.
- [8] Becker Th, Meissner H. Direct suction measurement in cyclic triaxial test Devices, Proceedings of 3rd International Conference on Unsaturated Soils, Recife, Brasil, 2002.
- [9] Becker T, Li T. Behavior of unsaturated soils subjected to cyclic loading, Proceedings of International Workshop on Unsaturated Soils, Weimar, Germany, Springer, 2003, pp. 347-364.
- [10] Mendoza CE, Colmenares JE, Merchan VE. Stiffness of an unsaturated compacted clayey soil at very small strains, Proceedings of an International Symposium On Advanced Experimental Unsaturated Soil Mechanics, Trento, Italy, 2005, pp.199-204.
- [11] Cabarkapa Z, Cuccovillo T. Automated Triaxial Apparatus for Testing Unsaturated Soils, Geotechnical Testing Journal, 2006, No. 1, Vol. 29.
- [12] Ng CWW, Yung SY. Determination of the anisotropic shear stiffness of an unsaturated decomposed soil, Géotechnique, 2008, No. 1, 58, pp. 23-35.
- [13] Pineda JA, Lima A, Romero EE. Influence of hydraulic path on the low-strain shear modulus of a stiff clay, Unsaturated Soils: Advances in Geo-Engineering, Taylor & Francis Group, London, 2008.
- [14] d'Onza F, d'Onofrio A, Mancuso C. Effects of unsaturated soil state on the local seismic response of soil deposits, Unsaturated Soils: Advances in Geo-Engineering, Taylor & Francis Group, London, 2008.
- [15] Ng CWW, Xu J, Yung SY. Effects of wetting-drying and stress ratio on anisotropic stiffness of an unsaturated soil at very small strains, Canadian Geotechnical Journal, 2009, Vol. 46, pp. 1062-1076.
- [16] Biglari M, Jafari MK, Shafiee A, Mancuso C, d'Onofrio A. Dynamic properties of unsaturated kaolin measured in a wide strain range with new suction controlled cyclic triaxial device, Geotechnical Testing Journal, ASTM, AIP ID: 001105GTJ, 2011.
- [17] Biglari M, d'Onofrio A, Mancuso C, Jafari MK, Shafiee A, Ashayeri I. Small-strain stiffness of Zenoz kaolin in unsaturated condition, Canadian Geotechnical Journal, 2012, Vol. 49, pp. 1-12.
- [18] Ng CWW, Xu J. Effects of current suction ratio and recent suction history on small-strain behaviour of an unsaturated soil, Canadian Geotechnical Journal, 2012, No. 2, Vol. 49, pp. 226-243.
- [19] Heitor A, Indraratna B, Rujikiatkamjorn C. Laboratory study of small-strain behavior of a compacted silty sand, Canadian Geotechnical Journal, 2013, No. 2, Vol. 50, pp. 179-188.
- [20] Suriol J, Romero E, Lloret A, Vaunat J. Small-strain shear stiffness of compacted clays: Initial state and microstructural features, Unsaturated Soils: Research & Applications, 2014, pp. 769-775.
- [21] Walton-Macaulay C, Bryson LS, Hippley BT, Hardin BO. Uniqueness of a constitutive shear modulus surface for unsaturated soils, ASCE, International Journal of Geomechanics, 10.1061/(ASCE) GM.1943-5622.0000470, 06015002, 2015.
- [22] Hilf JW. An Investigation of Pore Water Pressure in Compacted Cohesive Soils, Technical Memo, Bureau of 479 Reclamation, Denver, 1956.
- [23] Ladd RS. Preparing testing specimens using under-compaction, Geotechnical Testing Journal, 1978, pp. 16-23.
- [24] Sivakumar V. A Critical State Framework for Unsaturated Soils, Ph.D. thesis, University of Sheffield, Sheffield, U.K, 1993.